Second Order Sliding Mode Control of a STATCOM with Saturated Inputs*

Carlos A. Ruiz-Zea[1], Esteban Jiménez-Rodríguez[1], Juan D. Sánchez-Torres[2], José M. Cañedo Castañeda[1] and Alexander G. Loukianov[1]

***Abstract*— This paper presents a robust controller for a STATCOM device with saturated inputs. As the primary assumption, the proposed design considers the presence of unknown but bounded external perturbations and parametric variations. This proposal has a cascade structure, where a saturated super twisting control algorithm closes the currents control loop, and a high-gain proportional-integral (PI) algorithm ensures the voltage regulation. Thus, the exposed scheme provides an adequate performance of the STATCOM, considering the saturation of the inputs with the anti-windup feature. Posteriorly, a proper stability analysis presents the conditions for the appropriate operation of the closed-loop system in saturation and non-saturation regimes. Numerical simulations are also included to show the performance of the proposed controller.**

***Index Terms*— STATCOM, FACTS, Sliding Mode Control,Saturated Super Twisting, High Order PI.**

I. Introduction

The increased demand and the deregulation of electrical power systems often create transmission congestion scenarios and forced outages. Those conditions can induce undesirable effects as instability issues in the system. One solution to this problem is to improve the system capacity; however, this solution is not entirely viable due to its high economic and environmental cost [1]. On the other hand, an efficient and reliable solution is to incorporate devices which can handle dynamic disturbances such as loss generation, load rejection, and faults, so the preservation of the desired line voltage levels and the system stability.

In this sense, the implementation of flexible alternating current transmission systems (FACTS) arises as a promising solution. These devices are responsible for power systems compensation by maintaining bus voltages close to their nominal values, reducing line currents, and reducing system losses despite the disturbances mentioned before. One particular type of FACTS is the static synchronous compensator (STATCOM). This device is a shunt based on a voltage source converter (VSC) without a power source on the direct current (DC) side. Its function is to compensate the reactive power to increase the power transfer capacity in a transmission line by regulating the STATCOM output voltage magnitude. Hence, control objectives for the STATCOM are to supply a desired reactive power to the system and to maintain the DC voltage at a specific value [2].

In the last years, several researchers have developed plenty of control algorithms for the STATCOM. Among them, the proportional integral (PI) controllers have extensive use for this application [3]–[6]. However, since the STATCOM presents a nonlinear structure, the system's operating point may change in the presence of parametric variations or external disturbances. This major drawback makes difficult, sometimes impossible, to guarantee proper operation of the PI algorithms, other linear algorithms or linearization-based algorithms [7], [8].

At the same time, various nonlinear controllers have been proposed to improve the robustness of the closed-loop system. Some conventional approaches are the adaptive control [9], [10], the passivity-based control [11], [12], and the sliding-mode control (SMC) [13]–[16]. In this sense, considering the uncertainties and nonlinearities related to the mathematical model of the STATCOM, the SMC technique stands as a viable alternative due to its interesting features of robustness, insensitivity to parameter variations and external disturbances [17]–[19]. As examples, the reference [13] developed a sliding mode equivalent control-based controller for the STATCOM model. Here, the control design considers no variation in the system parameters. Similarly, the reference [14] proposed a cascade controller. For this case, a PI controller shapes the outer loop, while saturated linear controllers close the inner loops instead of relay controllers to prevent high frequency switching for PWM implementation. Again, the design assumes the full knowledge of the system parameters.

A remarkable case of nonlinear control for the STATCOM is the use second order SMC schemes [15], [16], as the well-known super-twisting algorithm [20]. One of the main advantages of that control strategy is its continuous nature, making easier the PWM implementation of the control signal. However, since the control signals for modulation must be between -1 and 1, the methods exposed by references [15], [16] need to include a saturation function. For those cases, this inclusion may represent a significant issue since it was not considered in the design of the inner loop but only for simulation and implementation aims. Consequently, the controller only assures its proper operation in the non-saturated zone and can produce undesirable windup effects in saturation regime. Furthermore, the design proposed in the work [16] presents differentiability

*This work was supported by CONACYT, México, under grant 252405.

[1]Department of Electrical Engineering, CINVESTAV-IPN Guadalajara, Av. del Bosque 1145 Col. El Bajío CP 45019, México. [caruiz,ejimenezr,josec,louk]@gdl.cinvestav.mx

[2]Research Laboratory on Optimal Design, Devices and Advanced Materials -OPTIMA-, Department of Mathematics and Physics, ITESO, Periférico Sur Manuel Gómez Morín 8585 C.P. 45604, Tlaquepaque, Jalisco, México dsanchez@iteso.mx

issues, since the constructed manifold includes the non-differentiable super twisting signal of the capacitor voltage regulation loop, making impossible to induce a sliding mode in the current loop applying another super twisting algorithm.

With the mentioned issues into consideration, this paper presents the design a robust controller for a STATCOM with saturated inputs, assuming the presence of unknown but bounded external perturbations associated to Load variation and magnitude of voltage variation. The saturated super twisting control algorithm [21], [22] is applied to design the currents control loop, and the high-gain PI algorithm [23] is used for the DC voltage regulation.

The main advantage of the proposed controller is the anti-windup feature. Furthermore, conditions for proper operation are derived, proving the adequate performance of the closed-loop system in saturation and non-saturation regimes, and in the presence of uncertainty produced for external disturbances and parametric variation.

II. Preliminaries

A. Saturated Super-Twisting Algorithm

Consider the first order perturbed system

$$\dot{\xi} = u + \phi, \tag{1}$$

where $\xi, \phi, u \in \mathbb{R}$, with ϕ a differentiable unknown perturbation. Assume that the perturbation term ϕ and its time derivative are globally bounded by $|\phi| \leq \phi_{\max}$, $|\dot{\phi}| \leq \Phi$. Moreover, the admissible control input for the plant is bounded, such that $|u| \leq \rho$, and continuous.

The control objective is to drive the system trajectory $\xi(t)$ to the origin $\xi = 0$ in finite time in spite of the perturbation term ϕ. It is immediate that for a bounded control input $|u| \leq \rho$ to be feasible, the allowed perturbations must satisfy $\phi_{\max} < \rho$.

A control law which satisfies the requirements mentioned above is the saturated super-twisting controller. It was proposed in [21], and has the following form:

$$\begin{bmatrix} u \\ \dot{z} \end{bmatrix} = \begin{cases} \begin{bmatrix} -\rho \operatorname{sign}(x) \\ 0, z(0) = 0 \end{bmatrix} & \text{if } s = 0 \\ \begin{bmatrix} -k_1 |x|^{1/2} \operatorname{sign}(x) + z \\ -k_2 \operatorname{sign}(x), z(0) = 0 \end{bmatrix} & \text{if } s = 1. \end{cases} \tag{2}$$

Note that the control law depends on the value of the binary variable s, which is set to $s = 0$ for every initial condition $\xi(0) = \xi_{10}$ outside the neighborhood $|\xi_{10}| > \delta > 0$. On the other hand, it is set to $s = 1$ if the state trajectory enters to (or begins in) the set $|\xi(t)| \leq \delta$, and keep this value ($s = 1$) for all future time, even if the state becomes $|\xi(t)| > \delta$.

The stability and robustness conditions of for the system (1) closed-loop with the saturated super-twisting controller (2) are given in the following proposition:

Theorem 1 ([21]): The origin $\xi = 0$ of the closed-loop system (1)-(2) is strongly globally asymptotically stable if the gains satisfy

$$\begin{aligned} k_1 &> 0 \\ k_2 &> 3\Phi + \frac{2\Phi^2}{k_1^2}, \end{aligned} \tag{3}$$

and the maximum allowed bound for the perturbation term also satisfies

$$\phi_{\max} \leq \frac{\kappa_1 \rho + \sqrt{\delta}\alpha_2 - \sqrt{\kappa_2}}{\kappa_1 - \alpha_3}, \tag{4}$$

where $\kappa_1 = \frac{\alpha_1\alpha_3 - \alpha_2^2}{\alpha_3 k_1^2 - 2\alpha_2 k_1 + \alpha_1}$, $\kappa_2 = (\alpha_2^2 + \kappa_1\alpha_1 - \alpha_1\alpha_3)\delta + 2\kappa_1\alpha_2\rho\sqrt{\delta} + \kappa_1\alpha_3\rho^2$, $\alpha_1 = k_2 + \frac{k_1^2}{2}$, $\alpha_2 = -\frac{k_1}{2}$, and $\alpha_3 = 1$.

Moreover, all trajectories $\xi(t)$ converge in a finite time $t_\phi > 0$ to the origin $\xi = 0$.

Remark 1 ([21]): The close to the origin the Super-Twisting behavior starts ($\delta \to 0$), the greater magnitude of the perturbation ($\phi_{\max}$) is allowed, and on the other hand, the far to the origin the Super-Twisting behavior starts the lesser magnitude of the perturbation is allowed.

B. High-Gain PI Algorithm

Consider again the system (1). In this case, the admissible control input can be unbounded but must be differentiable.

The control objective is to drive the system trajectory $\xi(t)$ to a vicinity of the origin $|\xi| < \kappa$, with $\kappa > 0$, in finite time despite the perturbation term ϕ.

A control law that match the constraints above is the linear high-gain PI algorithm [23], which is defined as

$$\begin{aligned} u &= -\rho\beta_1\xi + z \\ \dot{z} &= -\rho^2\beta_2\xi, \end{aligned} \tag{5}$$

where β_1 and β_2 are positive gains, and $\rho \geq 1$.

To analyze the effect of the controller (5) on the system (1), define the transformation $x_1 = \rho\xi$, $x_2 = z + \phi(t)$ and $\mathbf{x} = \begin{bmatrix} x_1 & x_2 \end{bmatrix}^T$, to get the linear perturbed system structure

$$\dot{\mathbf{x}} = \rho\mathbf{A}\mathbf{x} + \bar{\phi}, \tag{6}$$

where $\mathbf{A} = \begin{bmatrix} -\beta_1 & 1 \\ -\beta_2 & 0 \end{bmatrix}$ and $\bar{\phi} = \begin{bmatrix} 0 & \dot{\phi}(t) \end{bmatrix}^T$.

Now, consider the following quadratic Lyapunov function candidate for the closed-loop system (6)

$$V = \mathbf{x}^T\mathbf{P}\mathbf{x}. \tag{7}$$

where $\mathbf{P} \in \mathbb{R}^{2\times 2}$ is a symmetric positive definite matrix.

Remark 2: Since the matrix $\mathbf{A}$ is Hurwitz ($\beta_1, \beta_2 > 0$), there exists a unique solution $\mathbf{P}$ to the Lyapunov equation

$$\mathbf{A}^T\mathbf{P} + \mathbf{P}\mathbf{A} = -\mathbf{Q},$$

where $\mathbf{Q} \in \mathbb{R}^{2\times 2}$ is a symmetric positive definite matrix.

The following propositions present the stability and robustness of the high-gain PI controller:

Theorem 2: The solutions of system (1) closed-loop with (5) are globally ultimately bounded, with ultimate bound given by $\mu\sqrt{\frac{\lambda_{\max}(\mathbf{P})}{\lambda_{\min}(\mathbf{P})}}$, where $\mu = \frac{2\Phi||\mathbf{p}_2||_2}{\rho\theta\lambda_{\min}(\mathbf{Q})}$, $0 < \theta < 1$ and

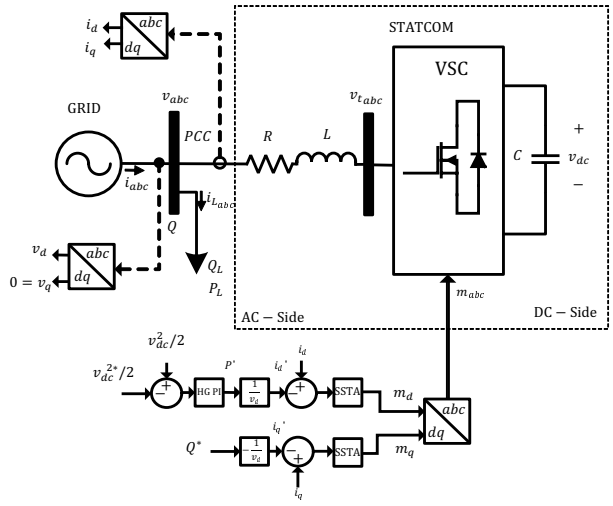

Fig. 1. Electrical System with STATCOM in Bus 1

$\mathbf{p}_2$ the second column of $\mathbf{P}$, i.e., there is a finite time t_1 such that $||\mathbf{x}(t)|| \leq \mu\sqrt{\frac{\lambda_{\max}(\mathbf{P})}{\lambda_{\min}(\mathbf{P})}}$ for all $t > t_1$.

The proof of this theorem is not given due to lack of space. However, it can be done following [24].

Remark 3: Since $\rho \geq 1$, for all $t > t_1$, $|\xi(t)| \leq ||\mathbf{x}(t)|| \leq \mu\sqrt{\frac{\lambda_{\max}(\mathbf{P})}{\lambda_{\min}(\mathbf{P})}}$.

III. Problem Statement

A. System Model

Figure 1 shows a control scheme which illustrates the STATCOM device interfaced to point of common coupling (PCC), where it is connected to a equivalent electrical power system represented by an ideal three-phase voltage source v_{abc}. The inductor L and the resistance R stand for the coupling transformer and the electrical losses of the link between the STATCOM and the VSC.

Additionally, the system model considers the following assumptions:

- Balanced conditions and constant frequency.
- Voltage of electrical system is constant.
- The system is assumed to be synchronized, and the reference frame direct axis is aligned to the direct component of the grid voltage. Thus, v_d is a DC value and $v_q = 0$.

The active and the reactive power at the PCC in dq frame are given respectively in p.u. values by $P = v_d i_d + v_q i_q$ and $Q = -v_d i_q + v_q i_d$. Hence, on PCC, the active and reactive powers are

$$\begin{aligned} P &= v_d i_d \\ Q &= -v_d i_q. \end{aligned} \tag{8}$$

With the above, the averaged dynamics of the system are written in dq frame to simplify the system analysis and controller design. The model of the system in p.u. is [2]

$$\begin{aligned} \frac{L}{\omega_b}\frac{di_d}{dt} &= -Ri_d + \omega L i_q - v_{dc}m_d + v_d + \phi_d \\ \frac{L}{\omega_b}\frac{di_q}{dt} &= -\omega L i_d - Ri_q - v_{dc}m_q + \phi_q \\ \frac{C}{\omega_b}\frac{dv_{dc}}{dt} &= i_d m_d + i_q m_q + f_{vdc} \end{aligned} \tag{9}$$

Where i_d and i_q are the input currents, v_{dc} is the dc capacitor voltage , v_d is the grid direct axis voltage, m_d and m_q are the modulation functions, ω and ω_b are the angular frequency of the system in p.u and based angular frequency respectively.
The functions ϕ_d, ϕ_q and f_{vdc} are given by

$$\begin{aligned} \phi_d &= \frac{L}{\omega_b}\frac{di_{Ld}}{dt} + Ri_{Ld} - \omega L i_{Lq} \\ \phi_q &= \frac{L}{\omega_b}\frac{di_{Lq}}{dt} + \omega L i_{Ld} + Ri_{Lq} \\ f_{vdc} &= -i_{Ld}m_d - i_{Lq}m_q, \end{aligned} \tag{10}$$

where i_{Ld} and i_{Lq} are the unknown load currents associated variation of $Q_L = -v_d i_{Lq}$ and $P_L = v_d i_{Ld}$.

B. Control Objectives

The main objective of a STATCOM devices is to compensate reactive power. Additionally, it may compensate the system power losses. Thus, the control objectives are

- to track a desired reactive power Q^*; from (8), this is done setting up a reference value for $i_q^* = -\frac{Q^*}{v_d}$ and tracking this desired current value $i_q \to i_q^*$;
- to regulate the dc capacitor voltage to a certain value $v_{dc} \to v_{dc}^*$.

IV. Control Design

A. DC Capacitor Voltage Regulation

Taking into account that, in general, the inductance value satisfies $L \ll 1$, the currents dynamics are much faster than the dc capacitor voltage dynamics. Hence, the dc capacitor voltage control design can be simplified using the singular perturbation theory [13], [19], [25]. Formally, we can let the left side of the first two equations of (9) tend to zero, solve algebraically for m_d and m_q, and replace into the third equation of (9) to get

$$\frac{C}{\omega_b}v_{dc}\frac{dv_{dc}}{dt} = \frac{C}{2\omega_b}\frac{dv_{dc}^2}{dt} = P^* - P_\delta(t), \tag{11}$$

where $P^* = v_d i_d^*$ is the desired active power, $P_\delta(t) = R((i_d^*(t) - i_{Ld})^2 + (i_q^*(t) - i_{lq}^2))$ is an unknown term associated with the losses of the converter, and i_d^* and i_q^* are the desired values of the direct axis and quadrature axis currents.

Here, P^* (or, equivalently, i_d^*) is regarded as a virtual control in equation (11). In this sense, we can say that v_{dc} has relative degree two with respect to m_d, which implies that P^* (i_d^*) must be designed to be differentiable.

Finally, P^* is designed as a high-gain PI algorithm (see Subsection II-B) as follows:

$$\begin{aligned} P^* &= -\rho_3 k_{31} e_3 + z_3 \\ \dot{z}_3 &= -\rho_3^2 k_{32} e_3, \end{aligned} \tag{12}$$

where $e_3 = \frac{1}{2}\left(v_{dc}^2 - (v_{dc}^*)^2\right)$, $k_{31}, k_{32} > 0$, and $\rho_3 \geq 1$. Here v_{dc}^* is a desired value of DC voltage capacitor.

B. Current Tracking

Defining $x = [x_1 \quad x_2 \quad x_3]^T = [i_d \quad i_q \quad v_{dc}]^T$ and $u = [u_1 \quad u_2]^T = [m_d \quad m_q]^T$, the model (9) can be expressed as

$$\begin{aligned} \dot{x}_1 &= f_1(x_1, x_2) + b(x_3)u_1 + \frac{\omega_b}{L}\phi_d \\ \dot{x}_2 &= f_2(x_1, x_2) + b(x_3)u_2 + \frac{\omega_b}{L}\phi_q \\ \dot{x}_3 &= x_1 u_1 + x_2 u_2 + f_{v_{dc}} \end{aligned} \tag{13}$$

where $f_1(x_1, x_2) = -\frac{R\omega_b}{L}x_1 + \frac{\omega_b \omega L}{L}x_2 + \frac{\omega_b}{L}v_d$, $f_2(x_1, x_2) = -\frac{\omega_b \omega L}{L}x_1 - \frac{R\omega_b}{L}x_2$, and $b(x_3) = -\frac{\omega_b}{L}x_3$.

At normal operating conditions, the dc capacitor voltage satisfies $x_3 \geq \bar{x}_3 > 0$ (i.e., the dc capacitor voltage x_3 is bounded below by a fixed and positive quantity $\bar{x}_3$). Thus, the function $b(x_3)$ is such that $|b(x_3)| \geq |b(\bar{x}_3)| := \bar{b} > 0$. Now, the current tracking errors are defined as $e_1 = x_1 - x_1^* = i_d - i_d^*$ and $e_2 = x_2 - x_2^* = i_q - i_q^*$, and their dynamics are obtained as

$$\begin{aligned} \dot{e}_1 &= b(x_3)u_1 + \phi_1 \\ \dot{e}_2 &= b(x_3)u_2 + \phi_2, \end{aligned} \tag{14}$$

where the perturbation terms $\phi_1 = f_1(x_1, x_2) - \dot{x}_1^* + \frac{\omega_b}{L}\phi_d$ and $\phi_2 = f_2(x_1, x_2) - \dot{x}_2^* + \frac{\omega_b}{L}\phi_q$, and its derivatives are assumed to be globally bounded by $|\phi_i| \leq \phi_{i,\max}$ and $\left|\dot{\phi}_i\right| \leq \Phi_i$.

Thus, the control signals u_1 and u_2 (modulation functions), are designed as saturated super twisting algorithms (see Subsection II-A) as follows:

$$\begin{aligned} u_i &= \frac{1}{b(x_3)}v_i \\ \begin{bmatrix} v_i \\ \dot{z}_i \end{bmatrix} &= \begin{cases} \begin{bmatrix} -\rho_i \text{sign}(e_i) \\ 0, z_i(0) = 0 \end{bmatrix} & \text{if } s_i = 0 \\ \begin{bmatrix} -k_{i1}\left|e_i\right|^{1/2}\text{sign}(e_i) + z_i \\ -k_{i2}\text{sign}(e_i), z_i(0) = 0 \end{bmatrix} & \text{if } s_i = 1, \end{cases} \end{aligned} \tag{15}$$

for $i = 1, 2$, where the gains $\rho_i = \bar{b}$, the gains k_{i1} and k_{i2} are selected as in Theorem 1. The binary variables s_i are set to $s_i = 0$ for initial conditions satisfying $|e_i(0)| > \delta_i > 0$. On the other hand, $s_i = 1$ if the state trajectory enters to (or begins in) the set $|e_i(t)| \leq \delta_i$, and keep this value for all future time. The bounds on the perturbation terms, $\phi_{i,\max}$, are assumed to satisfy (4).

Remark 4: From Subsection II-A, $|v_i| \leq \rho_i = \bar{b}$. Then, the above selection assures $|u_i| = \left|\frac{1}{b(x_3)}v_i\right| \leq \frac{\bar{b}}{|b(x_3)|} \leq 1$, which is a fundamental constraint on the modulation functions.

Remark 5: It is worth to notice that the controller presented in (12) and (15) only requires the knowledge of $b(x_3)$ from the model. Then, the robustness and the high performance of the controller despite the uncertainty of the model and its variations can be expected.

C. Stability Analysis

Replacing (15) in (14) it yields

$$\begin{aligned} \dot{e}_i &= v_i + \phi_i \\ \begin{bmatrix} v_i \\ \dot{z}_i \end{bmatrix} &= \begin{cases} \begin{bmatrix} -\rho_i \text{sign}(e_i) \\ 0, z_i(0) = 0 \end{bmatrix} & \text{if } s_i = 0 \\ \begin{bmatrix} -k_{i1}\left|e_i\right|^{1/2}\text{sign}(e_i) + z_i \\ -k_{i2}\text{sign}(e_i), z_i(0) = 0 \end{bmatrix} & \text{if } s_i = 1. \end{cases} \end{aligned}$$

Then, using Theorem 1, the origin $(e_1, e_2) = (0, 0)$ for the above closed-loop system is globally asymptotically stable, and the trajectories $(e_1(t), e_2(t))$ converge to the origin in a finite time $t_\phi = \max_{i \in \{1,2\}} t_{\phi_i}$.

Now, we analyze for $t > t_\phi$. Since $x_i = x_i^*$ ($i_d = i_d^*$ and $i_q = i_q^*$), from (11) and (12), the dynamics of $e_3 = \frac{1}{2}\left(v_{dc}^2 - (v_{dc}^*)^2\right) = \frac{1}{2}\left(x_3^2 - (x_3^*)^2\right)$ are

$$\begin{aligned} \frac{C}{\omega_b}\dot{e}_3 &= P^* - P_\delta(t) \\ P^* &= -\rho_3 k_{31} e_3 + z_3 \\ \dot{z}_3 &= -\rho_3^2 k_{32} e_3. \end{aligned}$$

Thus, using Theorem 2, the solutions of the above closed-loop system are globally ultimately bounded, i.e., $|e_3(t)| < \bar{\mu}$ for all $t > t_\phi + t_1$, where $\bar{\mu} > 0$ can be made arbitrarily small with an appropriate selection of ρ_3 (in fact, $\bar{\mu} \propto \frac{1}{\rho_3}$).

Remark 6: In Subsection IV-A, the voltage regulation loop is designed assuming $i_d = i_d^*$ and $i_q = i_q^*$ (or, equivalently $e_1 = 0$ and $e_2 = 0$). Note that in the Stability Analysis $(e_1, e_2) = (0, 0)$ in finite-time, because of the saturated super-twisting algorithm, assuring this assumption to hold.

V. Simulation results

Using parameters presented in Table I, numerical simulations are conducted for the closed-loop system (9), (12) and (15), using the Euler integration method with a fundamental step size of $1x10^{-6}$ s.

TABLE I
System Parameters

Parameter	Value	unit
ω_b	377	rad/sec
S_b	0.3	$MVAR$
v_b	391	V
v_{dc_b}	1200	V
ω	1	p.u
R	0.0043	p.u
L	0.0986	p.u
C	14.7929	p.u

The initial conditions of the state variables are set to $x_1(0) = 0.5$ p.u, $x_2(0) = -0.7$ p.u, $x_3(0) = 1.5$ p.u.The gains are selected as $\rho_i = 5730$, $k_{11} = 5000$ and the gains $k_{12} = 5x10^6$, $k_{21} = 1146$ and $k_{22} = 5730$, and $\rho_3 = 20$, $k_{31} = 1$ and $k_{32} = 1$. Furthermore, $\delta = 0.5$.

A simulation exercise is aimed to test the controller features of tracking the reactive power reference, DC voltage

regulation, and disturbance rejection. In this sense, the simulation includes the following changes:

- Q^* begins with 0 $p.u$ value, then it is set to $Q^* = -1$ $p.u$ at $t = 0.5$ s, then in $t = 1.5$ s $Q^* = 0.5$ $p.u$ and finally it is set to $Q^* = -1$ $p.u$ at $t = 2$ s.
- v_{dc}^* is kept constant at 1.54 $p.u$.
- Magnitude of v_d decrease from 1 $p.u$ to 0.9 $p.u$ at $t = 1.75$ s
- Q_L and P_L begins at 0 $p.u$ value, then in $t = 2.5$ s change to 0.3 pu respectively.

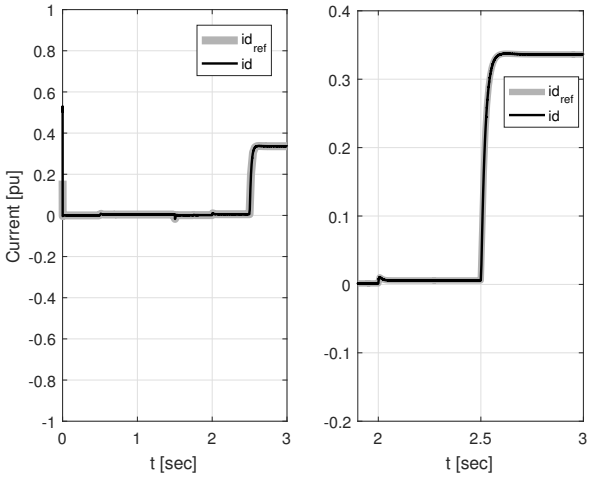

Fig. 2. Current on the direct axis

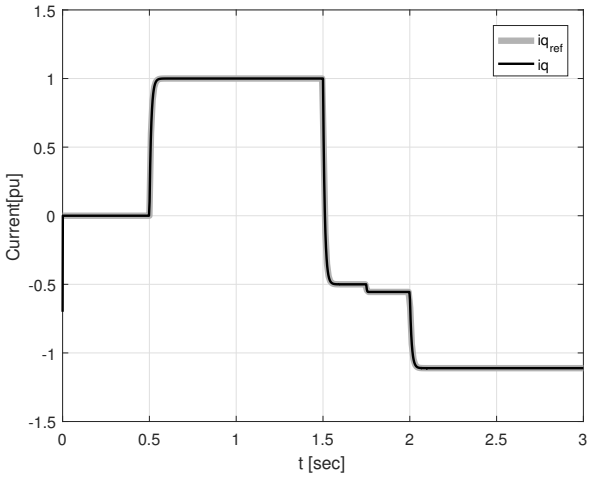

Fig. 3. Current on the quadrature axis

Figs. 2-5, show the variables of direct axis current $x_1 = i_d$, quadrature axis current $x_2 = i_q$, dc capacitor voltage $x_3 = v_{dc}$ and reactive power Q, together with their respective desired signals, respectively. Fig. 6 shows the control signals (modulation functions) $u_1 = m_d$ and $u_2 = m_q$. Based on these simulation results, it can be observed a good performance of the proposed controller, showing the features of saturation, quick response and robustness.

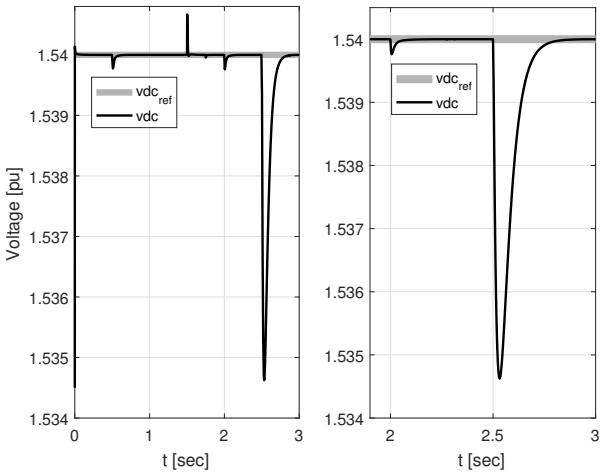

Fig. 4. dc Voltage

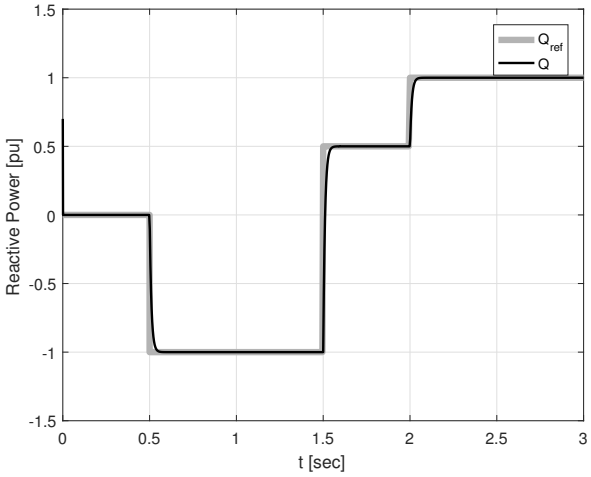

Fig. 5. Reactive power

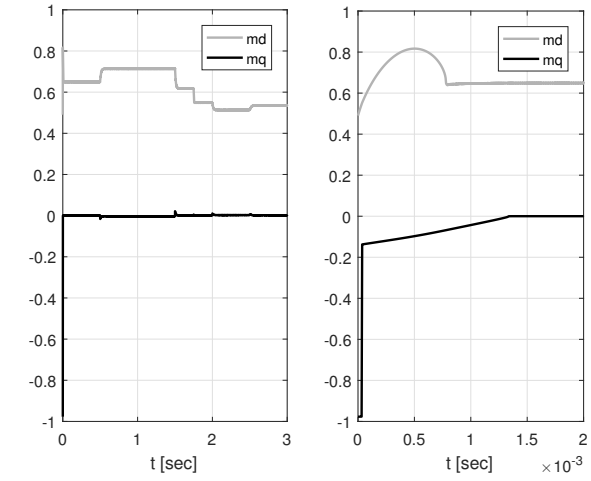

Fig. 6. Control Action

VI. Conclusions

This paper presented the design of a robust controller with saturated inputs for a STATCOM device. The proposed controller has a cascade structure, where the saturated super twisting controls the currents, while a high-gain PI algorithm regulates the DC voltage. In this sense, the designed controller assures the required performance considering the inputs saturation while maintaining the anti-windup feature.

The stability analysis was carried out, giving conditions for proper operation of the controller in saturation and non-saturation regimes are given. Numerical simulations were also included to show the performance of the proposed controller.

References

[1] X. Zhang, C. Rehtanz, and B. Pal, *Flexible AC Transmission Systems : Modelling and Control*, 2nd ed., Berlin, 2002.

[2] F. Shahnia, S. Rajakaruna, and A. Ghosh, *Static Compensators (STATCOMs) in Power Systems*, 2015.

[3] D. Soto and R. Pena, "Nonlinear control strategies for cascaded multilevel statcoms," *IEEE Transactions on Power Delivery*, vol. 19, no. 4, pp. 1919–1927, Oct 2004.

[4] M. S. El-Moursi and A. M. Sharaf, "Novel controllers for the 48-pulse vsc statcom and sssc for voltage regulation and reactive power compensation," *IEEE Transactions on Power Systems*, vol. 20, no. 4, pp. 1985–1997, Nov 2005.

[5] A. H. Norouzi and A. M. Sharaf, "Two control schemes to enhance the dynamic performance of the statcom and sssc," *IEEE Transactions on Power Delivery*, vol. 20, no. 1, pp. 435–442, Jan 2005.

[6] A. Jain, K. Joshi, A. Behal, and N. Mohan, "Voltage regulation with statcoms: modeling, control and results," *IEEE Transactions on Power Delivery*, vol. 21, no. 2, pp. 726–735, April 2006.

[7] A. Yazdani, M. L. Crow, and J. Guo, "A comparison of linear and nonlinear statcom control for power quality enhancement," in *2008 IEEE Power and Energy Society General Meeting - Conversion and Delivery of Electrical Energy in the 21st Century*, July 2008, pp. 1–6.

[8] A. Ghodousi and A. Jalilian, "A novel linear feedback control strategy for compensation of voltage flicker using statcom," in *2008 Joint International Conference on Power System Technology and IEEE Power India Conference*, Oct 2008, pp. 1–5.

[9] J. Linares-Flores, A. H. Méndez, C. García-Rodríguez, and H. Sira-Ramírez, "Robust nonlinear adaptive control of a boost converter via algebraic parameter identification," *IEEE Transactions on Industrial Electronics*, vol. 61, no. 8, pp. 4105–4114, Aug 2014.

[10] Y. Xu and F. Li, "Adaptive pi control of statcom for voltage regulation," *IEEE Transactions on Power Delivery*, vol. 29, no. 3, pp. 1002–1011, June 2014.

[11] Y. Gui, Y. O. Lee, Y. Han, W. Kim, and C. C. Chung, "Passivity-based control with nonlinear damping for statcom system," in *2012 IEEE 51st IEEE Conference on Decision and Control (CDC)*, Dec 2012, pp. 1715–1720.

[12] L. Harnefors, A. G. Yepes, A. Vidal, and J. Doval-Gandoy, "Passivity-based controller design of grid-connected vscs for prevention of electrical resonance instability," *IEEE Transactions on Industrial Electronics*, vol. 62, no. 2, pp. 702–710, Feb 2015.

[13] D. M. Vilathgamuwa, S. R. Wall, and R. D. Jackson, "Variable structure control of voltage sourced reversible rectifiers," *IEE Proceedings - Electric Power Applications*, vol. 143, no. 1, pp. 18–24, Jan 1996.

[14] F. Hamoud, M. L. Doumbia, and A. Cheriti, "Hybrid pi-sliding mode control of a voltage source converter based statcom," in *2014 16th International Power Electronics and Motion Control Conference and Exposition*, Sept 2014, pp. 661–666.

[15] J. Liu, S. Laghrouche, and M. Wack, "Observer-based higher order sliding mode control of power factor in three-phase ac/dc converter for hybrid electric vehicle applications," *International Journal of Control*, vol. 87, no. 6, pp. 1117–1130, 2014.

[16] J. Liu, S. Vazquez, L. Wu, A. Marquez, H. Gao, and L. G. Franquelo, "Extended state observer-based sliding-mode control for three-phase power converters," *IEEE Transactions on Industrial Electronics*, vol. 64, no. 1, pp. 22–31, Jan 2017.

[17] V. I. Utkin, *Sliding Modes in Control and Optimization*. Springer Verlag, 1992.

[18] S. V. Drakunov and V. I. Utkin, "Sliding mode control in dynamic systems," *Int. J. of Control*, vol. 55, pp. 1029–1037, 1992.

[19] V. I. Utkin, J. Guldner, and J. Shi, *Sliding Mode Control in Electro-Mechanical Systems, Second Edition (Automation and Control Engineering)*, 2nd ed. CRC Press, 5 2009.

[20] A. Levant, "Sliding order and sliding accuracy in sliding mode control," *International Journal of Control*, vol. 58, no. 6, pp. 1247–1263, 1993.

[21] I. Castillo, M. Steinberger, L. Fridman, J. A. Moreno, and M. Horn, "Saturated super-twisting algorithm: Lyapunov based approach," in *2016 14th International Workshop on Variable Structure Systems (VSS)*, June 2016, pp. 269–273.

[22] I. Castillo, M. Steinberger, L. Fridman, J. Moreno, and M. Horn, "Saturated super-twisting algorithm based on perturbation estimator," in *2016 IEEE 55th Conference on Decision and Control (CDC)*, Dec 2016, pp. 7325–7328.

[23] H. K. Khalil and L. Praly, "High-gain observers in nonlinear feedback control," *International Journal of Robust and Nonlinear Control*, vol. 24, no. 6, pp. 993–1015, 2014.

[24] H. K. Khalil, *Nonlinear Systems (3rd Edition)*, 3rd ed. Prentice Hall, 12 2001.

[25] F. Umbría, J. Aracil, F. Gordillo, F. Salas, and J. A. Snchez, "Three-time-scale singular perturbation stability analysis of three-phase power converters," *Asian Journal of Control*, vol. 16, no. 5, pp. 1361–1372, 2014. [Online]. Available: http://dx.doi.org/10.1002/asjc.818